Evaluating Wake Models for Wind Farm Control

Jennifer Annoni, Peter Seiler, Kathryn Johnson, Paul Fleming, and Pieter Gebraad

***Abstract*— Wind turbines are typically operated to maximize their own performance without considering the impact of wake effects on nearby turbines. There is the potential to increase total power and reduce structural loads by properly coordinating the individual turbines in a wind farm. The effective design and analysis of such coordinated controllers requires turbine wake models of sufficient accuracy but low computational complexity. This paper first formulates a coordinated control problem for a two-turbine array. Next, the paper reviews several existing simulation tools that range from low-fidelity, quasi-static models to high-fidelity, computational fluid dynamic models. These tools are compared by evaluating the power, loads, and flow characteristics for the coordinated two-turbine array. The results in this paper highlight the advantages and disadvantages of existing wake models for design and analysis of coordinated wind farm controllers.**

I. Introduction

Many states in the United States have set renewable portfolio standards that mandate renewable energy targets. For example, Minnesota has a target of 25% renewable energy by 2025 [1]. Wind energy is a fast growing source of renewable energy, hence it is a key component to meet these standards. Achieving these targets requires increasing the efficiency and reducing the overall costs of wind energy. In particular, increasing the power capture efficiency of existing wind farms is critical as suitable land for turbines is decreasing. In addition, reducing structural loads on turbines will improve the economic competitiveness of wind energy by reducing the operation and maintenance costs.

Currently, wind turbines are usually controlled individually to maximize their own performance. Many studies have shown that operating all turbines in a wind farm at their optimal operating point leads to suboptimal performance of the overall wind farm [2], [3], [4], [5], [6], [7], [8]. An improved understanding of the aerodynamic interactions between turbines can aid in the design of enhanced control strategies that coordinate all turbines in a farm. The papers cited above present coordinated turbine control strategies with the aim of increasing the total wind farm power and, in some cases, reducing the structural loads. The essential idea is that derating the lead turbine results in higher wind speeds for downstream turbines. Proper derating can result in a higher total power than simply operating each turbine at its own peak efficiency.

Most prior work on coordinated turbine control has used simplified actuator disk models for the design and analysis. More accurate wake modeling is necessary to help understand and quantify the aerodynamic interactions in a wind farm. A variety of wake models exist in literature that are useful for studying wind farm control. The simplest models are the Park model [9] and the eddy viscosity model [10]. These models provide a quick, preliminary description of the wake interactions in a wind farm. Also, there are various medium-fidelity tools, including the Dynamic Wake Meandering (DWM) model [11] and variations of the actuator disk model [12], [13], [14]. These medium-fidelity models give a more detailed description of the wake at a low computational cost. Finally, several high-fidelity computational fluid dynamics (CFD) models have been developed, e.g., [15], [16]. These high-fidelity models are the most accurate tools and can be used for evaluating wind farm controllers. However, they are computationally expensive.

In this paper, we investigate several wake models of varying fidelity and address their potential for control design and analysis for optimal wind farm performance. In order to highlight the features of the various wake models, the focus is restricted to the coordination of a two-turbine array aligned with the wind. As a result, yaw misalignment and the superposition of multiple wakes are not considered in this paper [17]. Section II formulates the coordinated control problem for the two-turbine array. This formulation includes a brief description of single turbine control and wake characteristics. Section III provides detailed descriptions for each wake model considered in this paper. The paper is not intended to compare all existing wake models. Instead, candidate models are selected for comparison based on the rough categorization of low, medium, and high fidelity. In addition, each of these models is available to the public. Section IV provides simulation results and comparisons using the selected wake models. The results highlight the advantages and disadvantages of each model. Finally, conclusions and suggestions for future work are given in Section V.

II. Wind Turbine Coordination

A. Single Turbine Operation

This section briefly reviews the operation and control of a single turbine. Additional details and references can be found in [18], [19], [20]. Utility-scale turbines have several inputs

Jennifer Annoni and Peter Seiler are with the Department of Aerospace Engineering & Mechanics, University of Minnesota. anno0010@aem.umn.edu and seiler@aem.umn.edu.

Kathryn Johnson is with the Division of Engineering, Colorado School of Mines and National Renewable Energy Laboratory kjohnson@mines.edu.

Paul Fleming is with the National Renewable Energy Laboratory Paul.fleming@nrel.gov.

Pieter Gebraad is with the Delft Center for Systems and Control, Delft University of Technology P.M.O.Gebraad@tudelft.nl.

*NREL's contributions to this work were supported by the U.S. Department of Energy under Contract No. DE-AC36-08GO28308 with the National Renewable Energy Laboratory. Funding for the work was provided by the DOE Office Energy Efficiency and Renewable Energy, Wind and Water Power Technologies Office.

that can be controlled to increase the captured power and reduce structural loads. For example, the turbine can yaw, or rotate, so that the turbine faces the wind direction. The power captured, P [W], from a single turbine is given by:

$$P = \frac{1}{2}\rho A u^3 C_P \tag{1}$$

where ρ [kg/m^3] is the air density, A [m^2] is the area swept by the rotor, u [m/s] is the wind speed perpendicular to the rotor plane, and C_P [unitless] is the power coefficient. The power coefficient is the fraction of available power in the wind captured by the wind turbine. C_P is a function of the blade pitch angle, β [rad], and the nondimensional tip-speed ratio (TSR), λ. TSR is defined as $\lambda = \frac{\omega R}{u}$, where ω [rad/s] is the rotor speed and R [m] is the rotor radius.

At low wind speeds, the objective of a turbine controller is to maximize power. This is done by maintaining an optimal blade pitch angle, β_*, and TSR, λ_*. The blade pitch angle is held fixed at β_*, and the generator torque is controlled to achieve λ_* in varying wind conditions. The generator torque, τ_g, can be computed from the standard control law:

$$\tau_g = K_g \omega^2 \tag{2}$$

where $K_g = \frac{C_P \rho A R^3}{2\lambda_*^3 N}$ and N is the gearbox ratio.

At or above rated wind speeds, the turbine controller holds the generator torque constant and pitches the blades to minimize structural loads. It is common to use a proportional-integral or proportional-integral-derivative controller for blade pitch control [18], [19].

The performance of a single turbine can be simulated using the FAST model developed by the National Renewable Energy Laboratory (NREL) [21]. FAST is a nonlinear simulation package that models the dominant structural modes for a wind turbine, e.g., tower and blade bending modes. In addition, the aerodynamic forces on the blade are modeled using blade element theory. FAST can determine the power production and loading characteristics experienced by a single turbine for a given wind profile. However, it does not include the capability to model the effect of the turbine on the airflow including downstream wakes.

B. Wake Characteristics

The wind turbine operation creates a trailing wake that can be divided into two regions: the near wake and the far wake (see Fig. 1). The near wake is defined as the region behind the turbine to 5 diameters downstream where characteristics of the flow field are dominated by the turbine geometry. Specifically, individual components of the turbine, such as the blades, have a larger impact, whereas further downstream the rotor diameter is more important as the smaller turbulent scales have averaged out. The flow in the near wake is driven by a strong nonzero pressure gradient and strong turbulence caused by tip vortices and separation of the flow at the blade edges. The tip vortices break down at about 4 diameters downstream, marking the transition from the near wake to the far wake. In the far wake, the pressure gradient becomes less significant, and the wake is less dependent on the turbine geometry and more on atmospheric and topographic effects. This region is approximately axisymmetric and self-similar, i.e., the wake at distances downstream take on a similar shape, making the wake easier to model [22].

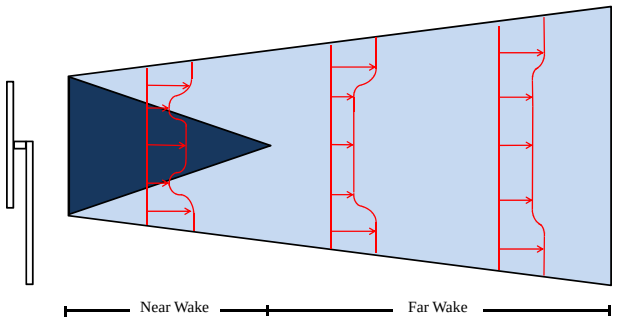

Fig. 1. Distinction between the near and far wake behind a wind turbine.

A model of the turbine interaction with the flow field is required to simulate the downstream wake. As previously noted, the standard implementation of the FAST simulation package does not include such a model. Two alternative models are considered in this paper. Both of these models can interface with FAST. The first model is an actuator disk [22]. This is a porous disk that can be modeled having constant, radial, or variable loading that influence the flow field. The advantage to using the actuator disk is that the blades of the turbine do not need to be modeled, which reduces the overall computation time. The second and more complex model is the actuator line [22]. This model takes finite sections of the rotating blade and calculates the airfoil lift and drag forces as they act on the flow. The lift and drag forces depend on the blade airfoil geometry and flow conditions. Nondimensional lift/drag data are typically stored in a look-up table as a function of the angle of attack between airflow and blade chord. This model can take considerably more computing time. Both the actuator disk and actuator line models can be used in CFD wake models.

C. Two-Turbine Coordination

This paper focuses on axial induction control for the two-turbine array shown in Fig. 2. Let P_1 and P_2 denote the power from Turbines 1 and 2, respectively. As described in Section II.A, the power generated by the first turbine depends on the inflow wind speed as well as the blade pitch β_1 and TSR λ_1 for the turbine. The inflow speed for the first turbine is approximately equal to the free-stream velocity, i.e., $u = U_\infty$, hence the power generated by Turbine 1 can be expressed as $P_1(\beta_1, \lambda_1, U_\infty)$. The operation of Turbine 1 disturbs the flow and this impacts the operation of the downstream turbine, i.e., Turbine 2. Specifically, the flow impacting the rotor on Turbine 2 depends on the blade pitch and TSR of Turbine 1. Thus the averaged power generated by Turbine 2 has a functional form of $P_2(\beta_1, \lambda_1, \beta_2, \lambda_2, U_\infty)$. The precise relationship describing the aerodynamic coupling between the turbines depends on the model used for the

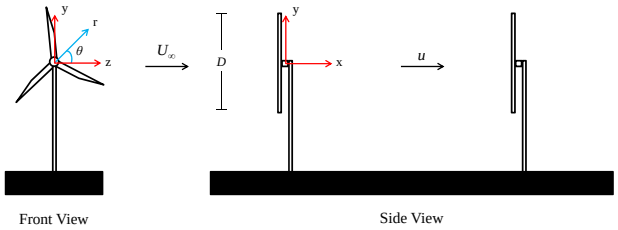

Fig. 2. Two-turbine setup for evaluating axial induction control using various wake models.

near/far wake. The total power generated by the two-turbine array is thus given by:

$$P_{tot}(\beta, \lambda, U_\infty) = P_1(\beta_1, \lambda_1, U_\infty) + P_2(\beta, \lambda, U_\infty) \quad (3)$$

where the vectors $\beta := [\beta_1, \beta_2]^T$ and $\lambda := [\lambda_1, \lambda_2]^T$ are defined to simplify the notation. The main objective of axial induction control is to maximize the total average power output:

$$\max_{\beta,\lambda} P_{tot}(\beta, \lambda, U_\infty) \quad (4)$$

This problem formulation assumes a constant free-stream velocity U_∞, which is essentially a steady-state formulation. A low-level generator torque control law can be used to regulate the turbine to the optimal TSR. A more realistic formulation treats the free-stream velocity as unsteady and turbulent. In this case, the objective is to maximize the average power generated by the two-turbine array. Moreover, the unsteady flow causes significant structural loads on the tower and blades of both turbines. Thus the formulation can be extended to include constraints on the loads. Alternatively, additional terms can be included in the objective function to trade off the power capture and loads.

The power maximization problem in (4) is difficult to solve as it involves complicated models of the turbine operation and wake interactions. As a result, previous work on turbine coordination [2], [3], [4], [5] has focused on simplified models for the turbine operation. In particular, the induction factor for a single turbine is defined as $a := 1 - \frac{u_1}{U_\infty}$, where u_1 denotes the average horizontal speed across the rotor plane. The turbine induction factor can be related to the power and thrust coefficient by the actuator disk theory [20]:

$$C_P(a) = 4a(1-a)^2 \quad (5)$$

$$C_T(a) = 4a(1-a) \quad (6)$$

The thrust coefficient is the ratio of the axial thrust force (perpendicular to the rotor plane) and the dynamic force on the rotor. The induction factor thus controls the power and thrust coefficient of a turbine and hence impacts the velocity deficit. Decreasing the power and thrust coefficient of the upstream turbine increases the velocity seen at the downstream turbine. Again, the precise relationship between the downstream wake and the induction factor of Turbine 1, a_1, depends on the wake model. Thus the power generated by a two-turbine array can potentially be increased by proper choice of the induction factors $a := [a_1, a_2]^T$. The power maximization problem formulated for this simplified turbine (actuator disk) model is given by:

$$\max_{a} P_{tot}(a, U_\infty) \quad (7)$$

The connections between the simplified and more realistic power maximization problems (4) and (7) are described further in Section IV.B.

III. Wake Models

Various wake models exist that range in fidelity and computational intensity. Each model can help strengthen the understanding of wakes in a wind farm.

A. Park Model

The simplest wake model is the Park model [9], [23]. This model has been widely used in wind farm control literature in recent years [2], [3], [5], [6]. The Park model has the lowest fidelity and requires the least computational time of the models considered in this paper. The turbine is modeled as an actuator disk with uniform axial loading in a steady uniform flow. This model is only valid for the far wake.

Consider the example of a turbine operating in a free-stream velocity U_∞ as shown in Fig. 2. The diameter of the turbine rotor plane is denoted by D and the turbine is assumed to be operating at an induction factor, a. A cylindrical coordinate system is placed at the rotor hub of the first turbine with the downstream and radial distances denoted by x and r, respectively. The velocity profile at a location (x, r) is:

$$u(x, r; a) = U_\infty(1 - \delta u(x, r; a)) \quad (8)$$

where the velocity deficit δu is given by:

$$\delta u = \begin{cases} 2a(\frac{D}{D+2kx})^2, & r \leq \frac{D+2kx}{2} \\ 0, & else \end{cases}. \quad (9)$$

In this model, the velocity, u, is defined in the axial (x) direction and the remaining velocity components are neglected. The wake is parameterized by a tuneable nondimensional wake decay constant k [24], [25].

The Park model can be used to compute the power production and velocity deficit of a turbine array. This is useful in determining operating conditions of a wind farm to maximize power. However, it has no notion of turbulence in the downstream wake and cannot determine the structural loads on the turbines. In addition, the assumptions are based on a steady inflow acting on an actuator disk with uniform axial loading. Despite its limitations, the Park model can be computed in seconds and can provide some insight of turbine interaction that can be used to understand the results obtained from higher-fidelity models.

B. Dynamic Wake Meandering Model

The next model considered is the medium-fidelity DWM model [11]. The University of Massachusetts and NREL developed an implementation of the DWM model that was originally created at the Technical University of Denmark [26]. It couples FAST with models for the wake deficit, turbulence, and (stochastic) meandering. The foundation of the wake deficit model used in the DWM model is the eddy viscosity model [10]. The wake deficit model numerically solves simplified Navier-Stokes equations based on the thin boundary-layer approximation and assumes a zero pressure gradient. Let x and r denote the downstream and radial distance from the turbine rotor hub as shown in Fig. 2. In this model, the velocity components, u and v, are defined in the axial (x) and radial (r) directions. The velocity components u and v satisfy the following partial differential equation:

$$u\frac{\partial u}{\partial x}+v\frac{\partial u}{\partial r}=-\frac{1}{r}\frac{\partial(r\overline{u'v'})}{\partial r} \tag{10}$$

The right-hand side of (10) can further be described in terms of turbulent viscosity, ϵ:

$$-(\overline{u'v'})=\epsilon\frac{\partial u}{\partial r} \tag{11}$$

where u' and v' denote the fluctuating velocity components in the axial and radial directions and $\overline{u'v'}$ is a temporal average that represents a turbulent momentum flux that acts like a stress, also known as a Reynolds stress. The turbulent viscosity, $\epsilon = k_2 b(U_\infty - u_c)$, describes the shear stresses and eddy viscosity in the wake, where b is the wake half width, u_c is the center wake velocity, and k_2 is an empirical constant of the flow field typically set to 0.009.

The DWM model uses Taylor's hypothesis when modeling turbulence. This hypothesis assumes that the turbulence has no effect on the wake advection, i.e., wake transport, from upstream to downstream. A consequence of this hypothesis is that the wake advection is only a function of the mean wind speed. The DWM model is interfaced with a FAST turbine model as follows. The first turbine is simulated in FAST with a three-dimensional input wind field. The DWM model is then used to calculate the downstream wake based on the FAST simulation results for Turbine 1. The downstream wake is then linearly superimposed on the wind field to generate the velocity conditions for the downstream turbine, i.e., Turbine 2. Finally, a FAST simulation is performed for Turbine 2 using this wake superimposed wind profile.

The advantage of the DWM model over the Park model is that it gives a more realistic representation of the far wake at a low computational cost. The DWM model can be used to compute the power production, velocity deficit, and structural loads of a turbine array. The turbines are modeled as actuator disks coupled with FAST and can handle steady and unsteady inflows. In addition, the DWM model can run in minutes on a desktop computer. The disadvantage of the DWM model is that it is not suitable for feedback control design because it calculates the wakes of a wind turbine array one at a time, i.e., it does not provide a continuous flow. This complicates the use of this model for dynamic wind farm control.

C. Actuator Disk Model

The actuator disk model considered in this paper solves the unsteady, axisymmetric Navier-Stokes equations by using the streamfunction (ψ) - vorticity (ω) formulation assuming the flow is incompressible and inviscid [12], [27]. Let (u, v) denote the axial and radial velocity components and (x, r) denote the downstream and radial distances. Vorticity can be defined as $\omega = \frac{\partial v}{\partial x} - \frac{\partial u}{\partial r}$ and the streamfunction can be defined in terms of the axial and radial velocity components: $\frac{\partial \psi}{\partial x} = rv$ and $\frac{\partial \psi}{\partial r} = -ru$. Under some additional technical assumptions, the Navier-Stokes equations are reformulated to the following governing equations:

$$\frac{\partial \omega}{\partial t}+\frac{\partial(u\omega)}{\partial x}+\frac{\partial(v\omega)}{\partial r}=-\frac{1}{\rho}\frac{\partial f_x}{\partial r} \tag{12}$$

$$\frac{\partial^2\psi}{\partial x^2}-\frac{1}{r}\frac{\partial\psi}{\partial r}+\frac{\partial^2\psi}{\partial r^2}=r\omega \tag{13}$$

where f_x is the volume force of the actuator disk on the flow in the axial direction. Equation 12 is the transport of vorticity. Equation 13 is the Poisson equation for the stream function. The velocity components (u, v) can be computed from (ψ, ω). The turbines are modeled as actuator disks with a specified volume force acting on the flow. For example, an elliptical force distribution, used in this paper, is given by:

$$f_x(r)=\frac{3}{2}\rho U_\infty^2 C_T\sqrt{1-\left(\frac{r}{R}\right)^2} \tag{14}$$

where C_T is the thrust coefficient and R is the radius of the turbine. These equations are solved using standard CFD methods [28].

The actuator disk model ignores viscous effects that are necessary for the velocity in the wake to recover far downstream. The power production and velocity deficit of a turbine array can be computed within minutes on a desktop computer.

D. Simulator of On/Offshore Wind Farm Applications (SOWFA)

SOWFA is a high-fidelity simulation tool that was developed at NREL to do offshore wind farm studies [16], [29], [30], [31], [32]. It can also be applied to land-based wind farms. SOWFA is a large-eddy simulation that is coupled with the FAST turbine model and based on the OpenFOAM open source toolbox.

SOWFA uses an actuator line model coupled with FAST to study turbines in the atmospheric boundary layer. SOWFA solves the three-dimensionial incompressible Navier-Stokes equations and transport of potential temperature equations, which take into account the buoyancy and Coriolis effects. The buoyancy effect is caused by the temperature flux in the atmosphere and the Coriolis effect is the result of the rotation of the Earth.

SOWFA performs three-dimensional calculations that can describe the steady and unsteady flow field. This information can be used to compute the power, velocity deficits, and loads at each turbine in a wind farm. This level of computation, with high-fidelity accuracy, takes on the order of days to run

on a cluster using a few hundred processors [33], [34]. As a result, it would take considerable effort to perform feedback control design for a wind farm with this model. However, it is the highest fidelity model considered in this paper, hence its use is most suitable for evaluating wind farm controllers.

IV. Results and Discussion

A. Simulation and Comparison of Wake Models

The wake characteristics of each model were compared by simulating a two-turbine setup (Fig. 2) over 1000 s. The simulated turbines have a 126 m diameter and a hub height of 90 m. The wind speed in all simulations has a mean of 8 m/s with 6% turbulence intensity.

Fig. 3 compares the spatially-averaged streamwise velocity profile of the two-turbine setup for each model. SOWFA is the highest fidelity model and has been validated against wind farm data [31], [32]. The Park and DWM model results match SOWFA in the far wake at distances greater than around 3D downstream. In addition, the Park model wake decay constant, $k = 0.45$, was tuned to obtain a best fit agreement with SOWFA in the far wake. The velocity deficit computed from the actuator disk model agrees with SOWFA at distances up to 3D downstream. The actuator disk model is invalid in the far wake because it assumes inviscid flow. It is important to note that the Park, DWM, and actuator disk model use an averaged actuator disk to represent the turbine. Tip vortices in the wake are not resolved and we cannot say anything definitive about their accuracy in the near wake. SOWFA implements an actuator line turbine model and is thought to give the closest representation of the near wake of the models presented in this paper.

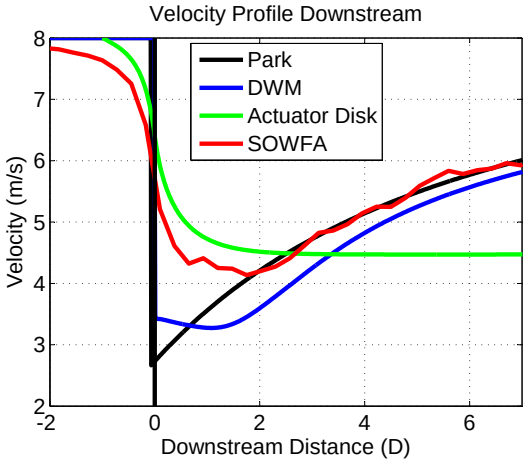

Fig. 3. Streamwise velocity component downstream of turbine.

Fig. 4 compares power production, power variance, and average tower fore-aft bending moments on the downstream turbine for each model. The results are presented for simulations with Turbine 2 placed with a downstream spacing of $x = 2D$ to $x = 7D$. The average power results are consistent with the velocity profiles shown in Fig. 3. At distances up to 3D downstream, the actuator disk model results align with SOWFA. However, the power of the actuator disk model remains constant far downstream because there is no wake recovery in the model. The DWM model follows SOWFA at turbine spacings of $4D$ and greater. These results correspond to cases where the downstream turbine is in the far wake of the upstream turbine. The Park model follows the same trend, but overestimates the power of the two-turbine array.

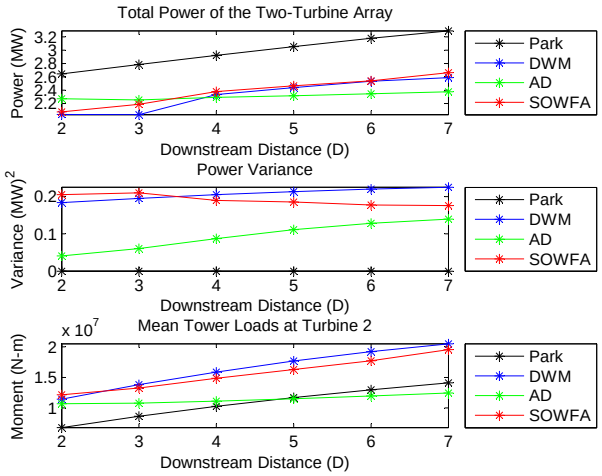

Fig. 4. Comparison of power, power variance, and tower loads generated from each wake model.

The middle subplot of Fig. 4 shows the power variance, and these results reflect the deviation in power over time. The Park model assumes steady flow and does not have a time component in the model. Thus, the variance for this model is identically equal to zero for all turbine spacings. The DWM and actuator disk models show an increase in power variance as the turbine spacing increases. This does not match the qualitiative trend of the SOWFA results, which show that the power variance decreases as the turbine spacing increases. The SOWFA results are more reasonable because turbulence decreases as the turbine spacing increases.

Finally, the bottom subplot of Fig. 4 shows the tower fore-aft bending moment that results from the axial (x direction) force on the turbine. The DWM model and SOWFA calculate this moment directly during the simulation. The Park model and the actuator disk model only model an overall axial thrust force on the turbine. The tower fore-aft moment can be approximated by multiplying the axial thrust force by the hub height of the turbine. The Park model, the DWM model, and SOWFA show an increase in the bending moment as the turbine spacing increases. The actuator disk model shows a relatively constant bending moment, which is caused by the lack of wake recovery in the model. The limitations in the Park model and the actuator disk model can be seen since both models can only provide a total axial force on a turbine. SOWFA and the DWM model are coupled with FAST, hence they provide a more accurate description of the tower loads.

B. Coordinated Control

This section provides results for two-turbine coordinated control on the Park, DWM, and actuator disk models. Section

II.C formulated power maximization problems with realistic (4) and simplified actuator disk (7) models for a single turbine. In both cases, the maximum power from the two-turbine array is obtained by operating the rear turbine at its peak efficiency. Thus, the optimization reduces to a determination of the optimal derating for the lead turbine. The Park model uses a 1D representation to model the turbines with an induction factor control input. The Park model is relatively simple, hence the optimal induction factor for the lead turbine a_1 can be determined numerically as previously demonstrated in [5].

Instead of optimizing the axial induction factor, the actuator disk model chooses a value of C_T^* for the front turbine that optimizes the power out of a two turbine array. The optimal induction factor for the actuator disk model can be computed from C_T^* using Eq. (6). The DWM model uses FAST to provide a more realistic turbine model and takes an input of blade pitch angle, β, and TSR, λ. The standard generator torque control law can be used to track the desired λ. After numerous open-loop runs at various (β, λ), the optimal (β^*, λ^*) of the first turbine can be approximately determined. This (β^*, λ^*) can be mapped to a C_P^* value using a software package, WT_Perf, developed at NREL [35]. The C_P^* can be related to the optimal induction factor using Eq. (5). Equations 5 and 6 are derived from simplistic models and are generally not realistic. However, they are close enough for axial induction factors to be compared across wake models. This approach only provides a suboptimal solution to the higher-fidelity power maximization problem. SOWFA also uses FAST to model the individual turbine dynamics, hence the approach described for the DWM model could also be used to generate control inputs for SOWFA.

Fig. 5 shows the results of axial induction control with various wake models. The Park model, with a tuned value of k, shows a decrease in power gained as the turbine spacing increases. The DWM model shows that there is an increase in power, but only for cases where the turbine spacing is less than 4 diameters. As the turbine spacing increases, there is more time for wake recovery. After a certain distance downstream of the turbine, the effects of axial induction control become less significant. The actuator disk model shows no improvement in the power of a two-turbine array when using axial induction control. Some simulations have been run in SOWFA at 4 and 7 diameter spacing. Although not shown, preliminary results in SOWFA show that there is very little power to be gained using axial induction control. This concept will need further investigation and validation.

C. Summary of Control Design and Analysis

Table 1 shows a summary of the models with some key components to consider when implementing wind farm control. The computation time represents the total time it took to run a simulation. The Park, DWM, and actuator disk models were run on a desktop computer. SOWFA was run on 256 cores at the Minnesota Supercomputing Institute. The last column specifies the turbine model implemented in each wake model.

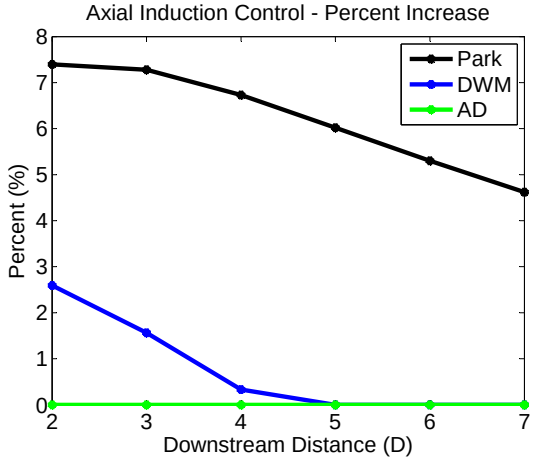

Fig. 5. Comparison of potential percentage of power gained by using axial induction control with different wake models

Model	Computation Time	Turbine Model
Park Model	5 seconds	One-dimensional
DWM	8 minutes	Actuator Disk
Actuator Disk	25 seconds	Actuator Disk
SOWFA	30 hours	Actuator Line

TABLE I
SUMMARY OF KEY CHARACTERISTICS OF EACH WAKE MODEL FOR 1000 SECOND SIMULATION.

The Park model is the fastest, simplest wake model and is suitable for feedback control. The induction factor is treated as the control input for a turbine in the Park model. By operating the first turbine at a suboptimal operating point, it may be possible to get more power out of the two-turbine array. Several studies have looked at this problem [2], [3], [4], [5], [6], [7], [13]. This model is only valid in the far wake, but gives an initial insight into how axial induction control might affect a two-turbine array.

The DWM model is a slower, but more complex model. It is harder to implement dynamic feedback control because the DWM model calculates the flow field for each turbine over its entire simulation time. The model inputs, blade pitch angle and generator torque, can be used to control the power coefficient of the first turbine. The benefit of using this model is that it can use individual turbine controllers with realistic inputs at a low computational cost.

The actuator disk model can be used in dynamic feedback control. The input to this model is the thrust coefficient. The thrust coefficient determines the loading on the actuator disk, which directly impacts the shape of the wake downstream.

Lastly, SOWFA is a high-fidelity simulation tool. It can be used for feedback control. Like the DWM model, the inputs to the turbine model are blade pitch angle and generator torque. Therefore, realistic turbine controllers can be

tested with SOWFA. However, large amounts of computing resources would be necessary. A few studies have been done with open-loop control in SOWFA [33], [34]. Each simulation in SOWFA can help validate the lower-fidelity models and evaluate wind farm controllers, which can provide a better understanding of the wake interactions associated with particular wind farm setups.

V. Conclusion and Future Work

There is potential for optimizing wind farm performance by coordinating turbine controllers. Coordinated control design requires accurate wake models with low computational cost. Low-fidelity models can provide useful insight into wake interaction, but lack the complexity to provide realistic wind farm results. Medium- and high-fidelity models are necessary for constructing an advanced controls framework that can be used to optimize turbine placement and control design in a wind farm. Future work will include evaluating these models using yaw control and looking at wake superposition in a wind farm with multiple rows and columns.

VI. Acknowledgments

The authors thank Matthew Lackner and Yujia Hao at the University of Massachusetts for their help in running simulations with the DWM model. This work was carried out in part using computing resources at the University of Minnesota Supercomputing Institute. This work was supported by the National Science Foundation under Grant No. NSF-CMMI-1254129 entitled CAREER: Probabilistic Tools for High Reliability Monitoring and Control of Wind Farms. Any opinions, findings, and conclusions or recommendations expressed in this material are those of the authors and do not necessarily reflect the views of the NSF.

References

[1] R. Wiser, "Renewable portfolio standards in the United States - a status report with data through 2007," LBNL-154E, Lawrence Berkeley National Laboratory, 2008.

[2] E. Bitar and P. Seiler, "Coordinated control of a wind turbine array for power maximization," in *American Control Conference*, pp. 2898–2904, 2013.

[3] P. M. O. Gebraad, F. C. van Dam, and J. W. van Wingerden, "A model-free distributed approach for wind plant control," in *American Control Conference*, pp. 628–633, 2013.

[4] K. E. Johnson and G. Fritsch, "Assessment of extremum seeking control for wind farm energy production," *Wind Engineering*, vol. 36, no. 6, pp. 701–716, 2012.

[5] K. E. Johnson and N. Thomas, "Wind farm control: Addressing the aerodynamic interaction among wind turbines," in *American Control Conference*, pp. 2104–2109, 2009.

[6] J. R. Marden, S. Ruben, and L. Pao, "A model-free approach to wind farm control using game theoretic methods," *IEEE Transactions on Control Systems Technology*, pp. 1207–1214, 2013.

[7] J. Schepers and S. Van der Pijl, "Improved modelling of wake aerodynamics and assessment of new farm control strategies," in *Journal of Physics: Conference Series*, vol. 75 012039, 2007.

[8] L. Machielse, S. Barth, E. Bot, H. Hendriks, and G. Schepers, "Evaluation of heat and flux farm control - final report," ECN-E–07-105, Energy Research Centre of the Netherlands (ECN), 2007.

[9] N. O. Jensen, "A note on wind generator interaction," Tech. Rep. Risø-M-2411, Risø, 1983.

[10] J. F. Ainslie, "Calculating the flowfield in the wake of wind turbines," *Journal of Wind Engineering and Industrial Aerodynamics*, vol. 27, no. 1, pp. 213–224, 1988.

[11] G. C. Larsen, H. Madsen Aagaard, F. Bingöl, J. Mann, S. Ott, J. N. Sørensen, V. Okulov, N. Troldborg, N. M. Nielsen, K. Thomsen, *et al.*, *Dynamic wake meandering modeling*. Risø National Laboratory, 2007.

[12] J. N. Sørensen and A. Myken, "Unsteady actuator disc model for horizontal axis wind turbines," *Journal of Wind Engineering and Industrial Aerodynamics*, vol. 39, no. 1, pp. 139–149, 1992.

[13] P. Torres, J.-W. van Wingerden, and M. Verhaegen, "Modeling of the flow in wind farms for total power optimization," in *Int. Conference on Control and Automation (ICCA)*, pp. 963–968, 2011.

[14] R. Mikkelsen, *Actuator disc methods applied to wind turbines*. PhD thesis, Technical University of Denmark, 2003.

[15] X. Yang and F. Sotiropoulos, "On the predictive capabilities of les-actuator disk model in simulating turbulence past wind turbines and farms," in *American Control Conference*, pp. 2878–2883, 2013.

[16] M. Churchfield and S. Lee, "NWTC design codes-SOWFA," *http://wind.nrel.gov/designcodes/simulators/SOWFA*, 2012.

[17] P. Gebraad, F. Teeuwisse, J. van Wingerden, P. Fleming, S. Ruben, J. Marden, and L. Pao, "A data-driven model for wind plant power optimization by yaw control," *Power [W]*, vol. 1, pp. 1–5.

[18] K. E. Johnson, L. Y. Pao, M. J. Balas, and L. J. Fingersh, "Control of variable-speed wind turbines: standard and adaptive techniques for maximizing energy capture," *Control Systems, IEEE*, vol. 26, no. 3, pp. 70–81, 2006.

[19] L. Y. Pao and K. E. Johnson, "Control of wind turbines," *Control Systems, IEEE*, vol. 31, no. 2, pp. 44–62, 2011.

[20] T. Burton, N. Jenkins, D. Sharpe, and E. Bossanyi, *Wind energy handbook*. John Wiley & Sons, 2011.

[21] J. Jonkman, "NWTC design codes - FAST," *http://wind.nrel.gov/designcodes/simulators/fast*, 2010.

[22] B. Sanderse, "Aerodynamics of wind turbine wakes," *Energy Research Center of the Netherlands (ECN), ECN-E–09-016, Petten, The Netherlands, Tech. Rep*, 2009.

[23] I. Katic, J. Højstrup, and N. Jensen, "A simple model for cluster efficiency," *EWEC*, pp. 407–410, 1986.

[24] T. Sørensen, M. L. Thøgersen, P. Nielsen, and N. Jernesvej, "Adapting and calibration of existing wake models to meet the conditions inside offshore wind farms," *EMD International A/S. Aalborg*, 2008.

[25] F. González-Longatt, P. Wall, and V. Terzija, "Wake effect in wind farm performance: Steady-state and dynamic behavior," *Renewable Energy*, vol. 39, no. 1, pp. 329–338, 2012.

[26] Y. Hao, M. Lackner, R.-E. Keck, S. Lee, M. Churchfield, and P. Moriarty, "Implementing the dynamic wake meandering model in the NWTC design codes," in *AIAA*, 2013.

[27] J. N. Sørensen and C. W. Kock, "A model for unsteady rotor aerodynamics," *Journal of wind engineering and industrial aerodynamics*, vol. 58, no. 3, pp. 259–275, 1995.

[28] O. Zikanov, *Essential computational fluid dynamics*. John Wiley & Sons, 2010.

[29] P. Fleming, P. Gebraad, M. Churchfield, S. Lee, K. Johnson, J. Michalakes, J.-W. van Wingerden, and P. Moriarty, "SOWFA + super controller user's manual," tech. rep., National Renewable Energy Laboratory (NREL), Golden, CO, 2013.

[30] P. Fleming, P. Gebraad, J.-W. van Wingerden, S. Lee, M. Churchfield, A. Scholbrock, J. Michalakes, K. Johnson, and P. Moriarty, "The SOWFA super-controller: A high-fidelity tool for evaluating wind plant control approaches," tech. rep., National Renewable Energy Laboratory (NREL), Golden, CO, 2013. Proc. of the EWEA 2013.

[31] M. J. Churchfield, S. Lee, J. Michalakes, and P. J. Moriarty, "A numerical study of the effects of atmospheric and wake turbulence on wind turbine dynamics," *Journal of Turbulence*, no. 13, pp. 1–32, 2012.

[32] M. J. Churchfield, S. Lee, P. J. Moriarty, L. A. Martinez, S. Leonardi, G. Vijayakumar, and J. G. Brasseur, "A large-eddy simulation of wind-plant aerodynamics," in *Proc. of 50th AIAA Aerospace Sciences Meeting*, pp. 9–12, 2012.

[33] P. Fleming, P. Gebraad, M. Churchfield, S. Lee, K. Johnson, J. Michalakes, J.-W. van Wingerden, and P. Moriarty, "Evaluating techniques for redirecting turbine wakes using SOWFA," 2013. Proc. of ICOWES.

[34] P. Fleming, P. Gebraad, M. Churchfield, S. Lee, K. Johnson, J. Michalakes, J.-W. van Wingerden, and P. Moriarty, "High-fidelity simulation comparison of wake mitigation control strategies for a two-turbine case," 2013. Proc. of ICOWES.

[35] A. Platt, "NWTC design codes WT-Perf," *http://wind.nrel.gov/designcodes/simulators/wtperf/*, 2012.